ISSN 0021-3640, JETP Letters, 2026, Vol. 123, No. 3, pp. 167–176. © The Author(s), 2026. This article is an open access publication.
Russian Text © The Author(s), 2026, published in Pis'ma v Zhurnal Eksperimental'noi i Teoreticheskoi Fiziki, 2026, Vol. 123, No. 3, pp. 187–197.

OPTICS
AND LASER PHYSICS

Reduction of Measurement Complexity at Rank Reduction for Tomography of Polarization Qutrits in the Natural Basis

D. R. Chupakhin[a,b], N. A. Borshchevskaya[a,b,*], B. I. Bantysh[b], K. G. Katamadze[c], S. P. Kulik[a], and Yu. I. Bogdanov[b]

[a] *Center for Quantum Technologies, Faculty of Physics, Moscow State University, Moscow, 119991 Russia*
[b] *National Research Center Kurchatov Institute, Moscow, 123182 Russia*
[c] *Technology Innovation Institute, 9639 Abu Dhabi, UAE*
**e-mail: bornad@quantum.msu.ru*

Received November 18, 2025; revised December 12, 2025; accepted December 12, 2025

Tomography of polarization qutrits in a measurement scheme in a natural polarization basis with a minimum number of tunable elements has been investigated. The information completeness of protocols for states of various ranks has been analyzed theoretically using the analysis of the information matrix and compressive tomography methods was carried out; the results have been confirmed experimentally. The existence of a protocol with five dimensions that provides a complete reconstruction of arbitrary (including mixed) states has been shown, and it has been found that schemes with a smaller number of dimensions provide the complete reconstruction of pure states. The obtained protocols demonstrate high accuracy of reconstructing test states under the conditions of a limited set of rotations of the measuring basis.

DOI: 10.1134/S0021364025610036

1. INTRODUCTION

Quantum information technologies are considered as one of the most promising ways to develop computing and communication [1, 2]. The basic unit of quantum information encoding is a qubit, but the transition to multidimensional systems already at the level of qutrits ($d = 3$) and ququarts ($d = 4$) can improve the efficiency and noise immunity of communication and computing protocols, as well as expand the functionality of devices [3–6]. Reliable operation of such protocols requires accurate diagnostics at all stages, i.e., measurement (tomography) of quantum states in the Hilbert space used.

An increase in dimensionality d leads to an increase in the required number of measurements: in particular, a set of $d + 1$ mutually unbiased bases can be used for a complete tomography of a mixed state of dimension d [7, 8]. At the same time, if the restrictions on the rank of the state are known in advance (for example, if the state is pure), the number of necessary measurements can be significantly reduced: this follows from both the results of tomography with a priori information [9], and methods of compressed sensing [10] and adaptive compressive tomography [11–13]. Both lower and upper bounds on the number of outcomes/bases [14, 15], as well as explicit constructions on a limited number of orthonormalized bases [16, 17], are known for pure states.

Meanwhile, practical implementation does not necessarily allow for arbitrary measurements; real schemes are often strictly limited by the class of available transformations (rotations) of the measuring basis. Therefore, the task of developing experimentally implemented measurement protocols and analyzing their information completeness under given constraints is a non-trivial research problem.

In this work, we consider the problem of developing a complete tomography protocol with a minimum number of measurements for quantum states of different ranks using the example of the polarization state of two photons in the same mode, which forms a polarization qutrit in the "natural" (standard) polarization basis $\{|HH\rangle, |HV\rangle, |VV\rangle\}$ [18–23], without ququart postselection. We analyze only protocols that can be implemented in the simplest measurement scheme with the minimum number of tunable elements.

In this work, we expand the ideas proposed in [24], where a single protocol and fully mixed quantum states were considered, to states of an arbitrary rank, which made it possible to propose new tomography protocols for qutrits in a pure state with a smaller number of measurements. In addition, the theoretical study is supplemented by consideration of the information completeness of the protocols under study.

The paper has the following structure. Section 2 presents the concept of the completeness of a quantum protocol and the methods of its analysis used in this

work. The tomography protocols under study are described in Section 3. Section 4 provides a diagram of the experimental setup on which the protocols were tested, confirming the validity and practical applicability of the proposed theoretical approach. Section 5 contains the main conclusions of this work.

2. CRITERIA FOR THE COMPLETENESS OF TOMOGRAPHY PROTOCOLS

For the tomography of an unknown quantum state, a certain set of measurements is made, called a tomography protocol, and the parameters of the quantum state are then reconstructed from the measurement results. We will consider protocols consisting of a complete set of basic measurements. Each such measurement gives one of the d outcomes (where d is the dimension of the system), which are enumerated with an index i. In order to unambiguously reconstruct the parameters of the quantum state, it is necessary to carry out measurements in several bases specified with the index β.

The probability of observing the outcome i in the protocol measurement β is denoted by $p_{\beta,i} = \mathrm{Tr}(P_{\beta,i}\rho)$, where $P_{\beta,i}$ is the corresponding projector. Then the following matrix equation can be constructed:

$$p = B\mathrm{vec}(\rho). \tag{1}$$

Here, p is the column consisting of probabilities $p_{\beta,i}$, B is the matrix whose rows consist of matrix elements of the projector matrices $P_{\beta,i}$, and $\mathrm{vec}(\rho)$ is the operation of pulling the density matrix ρ into a column.

According to [14, 16, 25], an informationally complete protocol is a protocol that makes it possible to reliably distinguish any two states, i.e.,

$$\forall \rho^A, \rho^B \in \mathcal{S},$$
$$\begin{cases} p^A_{\beta,i} = \mathrm{Tr}(\rho^A P_{\beta,i}), \\ p^B_{\beta,i} = \mathrm{Tr}(\rho^B P_{\beta,i}), \Rightarrow \rho^A = \rho^B. \\ p^A_{\beta,i} = p^B_{\beta,i}, \end{cases} \tag{2}$$

Here, S is in the general case the total Hilbert space of quantum states, but in the case of some a priori information about the state, for example, a limit on its rank r, this set can be narrowed down to S_r.

For qutrits with the rank $r = d$, where d is the dimension of space (in the case of qutrits under consideration $d = 3$), the necessary and sufficient criterion for the information completeness of the protocol is the absence of zero singular elements of the matrix B in Eq. (1). For $r < d$, this criterion is only sufficient. However, the condition proposed in [26] can be used as necessary. According to this condition, if the information matrix does not have exactly r^2 zero eigenvalues, the protocol is considered incomplete. In this case, the information matrix itself is set in the form (see Appendix B)

$$H = 2n\sum_{\kappa}\frac{(\Lambda_\kappa|c\rangle)(\Lambda_\kappa|c\rangle)^\dagger}{\gamma_\kappa}, \tag{3}$$

where n is the sample size, $|c\rangle$ is the purified state vector, $\gamma_\kappa = \langle c|\Lambda_\kappa|c\rangle$ is the probability of the outcome κ, and $\Lambda_\kappa = [P_{\beta,i}]^\dagger_\kappa [P_{\beta,i}]_\kappa$ is the process intensity operator. This means that if the qutrit state is reconstructed with rank 1 (as a pure state), 2 (partially mixed), and 3 (fully mixed), the information matrix must have exactly one, four, and nine zero eigenvalue, respectively, for the protocol can be informationally complete.

A sufficient condition for the completeness of the tomography protocol for a given rank is presented in [11–13], where the method of adaptive compressive tomography is described. The essence of the approach is as follows. First, some state ρ_r is randomly selected from the entire set S_r of quantum states of a given rank r (the method for generating a random state of a given rank is described in Appendix B). Then, the probabilities $\{p_{\beta,j}\}$ of all outcomes are calculated for the selected state and the protocol under study. Further, the set of quantum states S_p that have the same set of probabilities in the measurements is considered. For each state from this set, the average value of some observable, determined by a random Hermitian matrix Z, can be calculated as $f(\rho) = \mathrm{Tr}\{Z\rho\}$. Then, the parameters of the state $\rho_r \in S_p$ are varied to maximize and minimize this function (thus obtaining the values $f_{\max}$ and $f_{\min}$, respectively). For the numerical implementation of convex optimization problems, we use the CVXPY package [27], where we use the splitting conic solver (SCS) algorithm with the accuracy $\epsilon = 10^{-6}$ as an optimizer, which is suitable for solving convex optimization problems.

The criterion for the completeness of the protocol under study is the proximity to zero of the function $S_{\mathrm{cvx}} = (f_{\max} - f_{\min})/(f_{\max,1} - f_{\min,1})$, where $f_{\max,1}$ and $f_{\min,1}$ are calculated for a reduced protocol consisting of only one (first) measurement. In fact, it follows from the condition $S_{\mathrm{cvx}} = 0$ that the states that satisfy the measured probability values and minimize and maximize the function f (let they be denoted as $\rho_{\max}$ and $\rho_{\min}$, respectively) coincide with each other, which means that the measured probabilities allow one to uniquely reconstruct the quantum state and the protocol is complete. In order to explicitly check the coincidence of the states $\rho_{\max}$ and $\rho_{\min}$, along with S_{cvx}, the accuracy of the reconstruction (fidelity) $F(\rho_{\max}, \rho_{\min})$ was also calculated by the formula

$$F(\rho_1,\rho_2) = \left(\mathrm{Tr}\left\{\sqrt{\sqrt{\rho_1}\rho_2\sqrt{\rho_1}}\right\}\right)^2. \tag{4}$$

This analysis was performed for 500 different randomly selected states ρ_r, and the maximum value $S_{cvx}^{(max)}$ and the minimum value $F_{cvx}^{(min)}$ (worst case) were determined for each protocol.

3. ANALYSIS OF THE COMPLETENESS OF THE PROTOCOLS FOR MEASURING QUTRIT IN THE NATURAL BASIS

We consider tomography protocols based on the scheme for measuring qutrits in the natural basis introduced in [24] (see Fig. 1). Its main advantages are easy implementation and minimization of the number of polarizing elements. The qutrit state $|\psi\rangle$ is transformed by a set of polarization elements, which is described by a unitary matrix U; after that, the measurement is carried out in the natural basis $\{|HH\rangle, |HV\rangle, |VV\rangle\}$ as follows: photons fall on a polarizing beamsplitter, where detectors are installed in the output channels to distinguish the number of photons. If the detector D_H has recorded a pair of photons, this corresponds to the projection on the state $|HH\rangle$; if the detector D_V has recorded a pair of photons, this corresponds to the projection on the state $|VV\rangle$; and if each detector has recorded one photon, this corresponds to the projection on the state $|HV\rangle$.

The transformation of the qutrit state with complex amplitudes c_{HH}, c_{HV}, and c_{VV} by the polarizing element described by the unitary matrix $U = \begin{pmatrix} w & v \\ -v^* & w^* \end{pmatrix}$ has the form [18, 21, 24]

$$\begin{pmatrix} c_{HH\text{out}} \\ c_{HV\text{out}} \\ c_{VV\text{out}} \end{pmatrix} = \begin{pmatrix} w^2 & \sqrt{2}wv & v^2 \\ -\sqrt{2}wv^* & |w|^2 - |v|^2 & \sqrt{2}w^*v \\ v^{*2} & -\sqrt{2}w^*v^* & w^{*2} \end{pmatrix} \begin{pmatrix} c_{HH\text{in}} \\ c_{HV\text{in}} \\ c_{VV\text{in}} \end{pmatrix}. \quad (5)$$

A particular case of such a polarizing transducer is a phase plate WP(δ, α) that introduces the phase difference δ and is rotated at the angle α, for which $w = \cos(\delta) + i\sin(\delta)\cos(2\alpha)$ and $v = i\sin(\delta)\cos(2\alpha)$.

The protocols under study involve the half-wave (HWP), quarter-wave (QWP), and eighth-wave (EWP) phase plates described by the respective transformations

$$\begin{aligned} \mathrm{HWP}(\alpha) &= \mathrm{WP}(\pi, \alpha), \\ \mathrm{QWP}(\alpha) &= \mathrm{WP}(\pi/2, \alpha), \\ \mathrm{EWP}(\alpha) &= \mathrm{WP}(\pi/4, \alpha). \end{aligned} \quad (6)$$

Protocols A5 and A4 with the quarter-wave plate. We start with the protocol previously proposed in our work [24]. It includes five measurements with one quarter-wave plate installed at angles 0, π/8, 3π/8, 5π/8, and 7π/8 and will be referred to as A5. Similarly, all subsequent protocols will be denoted by a letter with a number corresponding to the number of measurements.

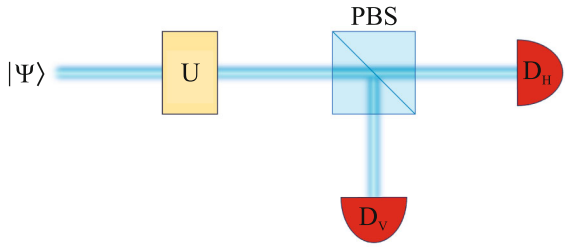

Fig. 1. (Color online) Diagram of tomography of the polarization qutrit in the natural basis. The radiation under study is divided into two channels by a polarizing beamsplitter PBS, and detectors D_H and D_V installed in each channel distinguish the numbers of horizontally and vertically polarized photons, respectively. For measurement in different bases, a polarizing element U is installed in front of the polarizing beamsplitter.

As established in [24], all singular values of the matrix B of this protocol are positive; consequently, this protocol is informationally complete for the reconstruction of qutrit states of any rank from pure to completely mixed. Compressive tomography calculations also showed that it satisfies the sufficient criterion of information completeness.

Analyzing the protocol A5 for rank-1 states, we obtained the S_{cvx} and F_{cvx} values presented in Fig. 2. It can be seen that $S_{cvx} = 0$ at $m = 4$, indicating that this protocol can retain information completeness even with the exclusion of the last measurement, which is further verified on experimental data. Similar plots were obtained if the last measurement 0, π/8, 5π/8, and 7π/8 was chosen. As an example, the protocol A4, where the QWP(π/8) measurement was discarded, is presented in Table 1 and Fig. 3.

Protocol B4 with the eighth-wave plate. Next, we analyze the protocol presented in [28], designating it as B4. It can be transformed into four measurements in the natural basis (see Fig. 1), which correspond to the following polarization transformations of the qutrit U: (i) identity transformation I corresponding to the measurement in the basis $\{|H\rangle, |V\rangle\}$, (ii) HWP(π/8) corresponding to the measurement in the basis $\{|D\rangle, |A\rangle\}$, (iii) HWP(π/8)EWP(0), and (iv) EWP(π/4). For this protocol, we derived an analytical relationship between the probabilities of different measurement outcomes and the coefficients describing the pure qutrit state, which proves its completeness for rank-1 states. This is also confirmed by the compressive tomography analysis of completeness.

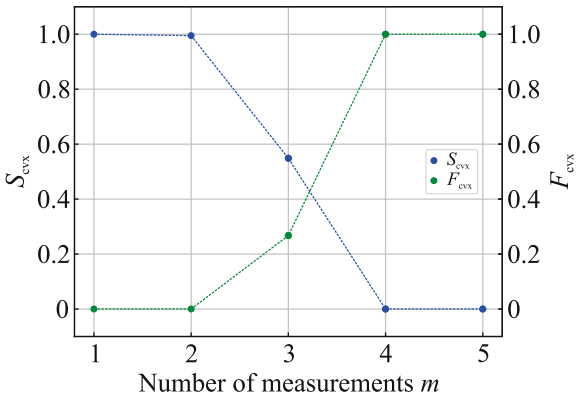

Fig. 2. (Color online) Quantities S_{cvx} and F_{cvx} plotted versus the number of measurements m for the corresponding set of angles 0, π/8, 3π/8, 5π/8, and 7π/8 to analyze the completeness of the protocol A5 and its reduced variants, for which only the first m measurements are used for the state of rank 1.

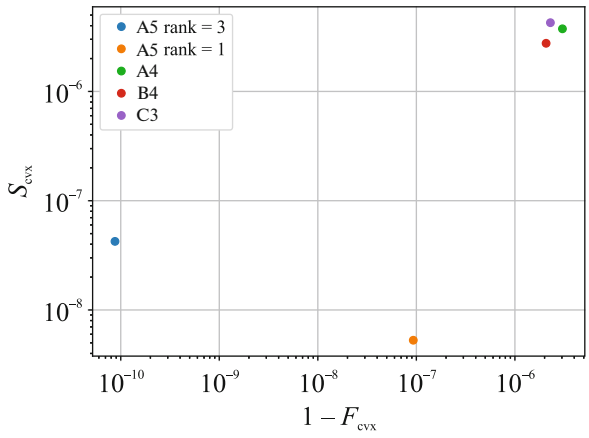

Fig. 3. (Color online) Values S_{cvx} and F_{cvx} for the protocols under study.

Optimal protocol C3 with the eighth-wave plate. We have also developed a protocol with the minimum number of measurements for the reconstruction of the qutrit in a pure state. It includes only three positions of the λ/8 plate at the angles π/3, π/8, and π/16 and also satisfies the sufficient criterion of completeness. For clarity, the S_{cvx} and F_{cvx} values demonstrating the sufficient condition for the completeness of all the protocols under study are presented in Fig. 3. The complete description of all protocols and their parameters is also given in the summary Table 1.

The summary S_{cvx} and F_{cvx} values in Fig. 3 and Table 1 provide a guideline for protocol selection based on the intended rank and the desired number of measurements. These theoretical estimates are further compared to the fidelity experimental values in Section 4.

It should be noted that all protocols also satisfy the necessary criterion of completeness [26].

4. EXPERIMENTAL APPROBATION OF THE PROTOCOLS

For the experimental approbation of the protocols under study, the same setup was used as in [24]; its dia-

Table 1. Comparative table of the protocols under study

Protocol	Theoretical description	Experimental implementation	Rank	$S_{cvx}^{(max)}$	$1 - F_{cvx}^{(min)}$	$\langle F_{exp} \rangle$
A5	QWP at angles 0, π/8, 3π/8, 5π/8, and 7π/8	QWP at angles 0, π/8, 3π/8, 5π/8, and 7π/8	1	4.2×10^{-9}	8.6×10^{-8}	0.9935
			3	9.8×10^{-8}	7.7×10^{-11}	0.9807
A4	QWP at angles 0, 3π/8, 5π/8, and 7π/8	QWP at angles 0, 3π/8, 5π/8, and 7π/8	1	4.3×10^{-6}	3.6×10^{-6}	0.9851
B4	(i) identity transformation (ii) HWP(π/8) (iii) HWP(π/8)EWP(0) (iv) EWP(π/4)	(i) HWP(0) (ii) HWP(π/8) (iii) HWP(π/8)QWP(−π/4) HWP(π/16)QWP(−π/4) (iv) Same as (iii) but with replaced input states[a]	1	2.6×10^{-6}	2.1×10^{-6}	0.9940
C3	(i) EWP(π/3) (ii) EWP(π/8) (iii) EWP(π/16)	(i) QWP(π/12)HWP(π/48)QWP(π/12) (ii) QWP(3π/8)HWP(7π/16)QWP(3π/8) (iii) QWP(5π/16)HWP(3π/8)QWP(5π/16)	1	3.2×10^{-6}	3.6×10^{-6}	0.9950

[a]To implement measurement (iv), the results of measurement (iii) were taken with the following replacement of the input states: $\phi_1 \leftrightarrow \phi_4$, $\phi_2 \leftrightarrow \phi_3$, $\phi_5 \leftrightarrow \phi_6$, and $\phi_7 \leftrightarrow \phi_8$.

gram is presented in Fig. 4. The setup allows one to prepare and reconstruct the following set of test states:

$$
\begin{aligned}
&|\phi_1\rangle = |HH\rangle, \quad |\phi_2\rangle = |VV\rangle,\\
&|\phi_3\rangle = |AA\rangle, \quad |\phi_4\rangle = |DD\rangle,\\
&|\phi_5\rangle = |RR\rangle, \quad |\phi_6\rangle = |LL\rangle,\\
&|\phi_7\rangle = \frac{1}{\sqrt{2}}(|HH\rangle - \mathrm{i}|VV\rangle),\\
&|\phi_8\rangle = \frac{1}{\sqrt{2}}(|DD\rangle + \mathrm{i}|AA\rangle),\\
&|\phi_9\rangle = \frac{1}{\sqrt{2}}(|RR\rangle - \mathrm{i}|LL\rangle).
\end{aligned}
\tag{7}
$$

The density matrices of these states form the basis in space of all qutrit density matrices; i.e., any mixed state ρ can be represented as the sum

$$\rho = \sum_{j=1}^{9} a_j |\phi_j\rangle\langle\phi_j|, \tag{8}$$

where a_j are the real decomposition coefficients. Thus, the possibility of reconstructing these states proves the possibility of using the tomography protocol for all possible quantum states of a given rank.

A detailed description of the scheme can be found in [24]. The only difference is that in the measuring part, phase plates installed at different angles were used as the U element, in accordance with the description of the examined protocols. In the absence of the λ/8 phase plate, equivalent combinations of half- and quarter-wave plates were used, see details in Table 1.

To reconstruct a quantum state, we used the maximum likelihood method together with the root parameterization of the density matrix (see Appendix A). Root parameterization makes it possible to choose the rank r of the density matrix. In particular, the choice $r = 1$ allows one to optimize the likelihood function only for a set of pure quantum states. The accuracy of the preparation of quantum states is determined by Eq. (4).

In the course of the experiment, each of the nine basic states (7) was prepared. For each state at each protocol measurement, ten repetitions were performed with an accumulation time of 30 s, which corresponds to the sample size ~10^4. The fidelity value F_{exp} was calculated by Eq. (4) between the density matrices of the prepared and reconstructed states.

The F_{exp} values obtained during the reconstruction of all nine pure states with each of the protocols are summarized in Fig. 6 and in Table 2 and the average values are given in Table 1. Fidelity values for all protocols are not lower than 0.97, which indicates that any of the protocols can be used. At the same time, protocols with fewer measurements show higher values of reconstruction accuracy, which indicates the dominant contribution of systematic rather than statistical errors to the overall error of reconstruction. In other words, the statistical component of the error with the selected sample size is already small compared to systematic effects, such as imperfect alignment of optical elements and slow drift of the setup parameters over time. In this case, a decrease in the number of measurements and, as a consequence, a decrease in the total time of the experiment lead to a decrease in the accumulation of systematic errors and, accordingly, to an increase in the observed accuracy of reconstruction for reduced protocols. It should be noted that such dependence of the accuracy of reconstruction on the number of measurements is due to the peculiarities of the relation between the statistical and systematic errors under the considered experimental conditions and should not be interpreted as a general rule for any protocols.

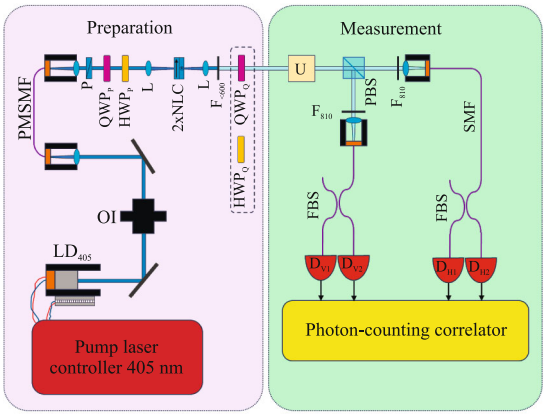

Fig. 4. (Color online) Diagram of the experimental setup for the preparation and tomography of polarization qutrits in a natural basis: (LD_{405}) narrowband laser diode at a wavelength of 405 nm, (DG) diffraction grating, (OI) optical isolator, (PMSMF) polarization-maintaining single-mode optical fiber, (P) polarizer, (L) lens, (2xNLC) a pair of 0.5-mm-thick nonlinear optical BiBO crystals with crossed optical axes, ($F_{<600}$) filter blocking radiation with a wavelength less than 600 nm, (F_{810}) filter centered on a wavelength of 810 nm with a width of 10 nm, (QWP_P, QWP_Q) quarter-wave phase plates, (HWP_P, HWP_Q) half-wave phase plates, (PBS) polarizing beamsplitter, (U) corresponding protocol transformation, (SMF) single-mode optical fiber, (FBS) 50:50 fiber beamsplitters, and (D_{H1}, D_{H2}, D_{V1}, D_{V2}) single-photon detectors based on silicon avalanche photodiodes.

In addition, the possibility of mixed-state tomography using the protocol A5 was investigated. First, we reconstruct pure states $\{|\phi_j\rangle\}$ using a state model of rank 2 and 3. The results are summarized in Table 2. It can be seen that the average reconstruction accuracy with the rank-2 model decreases from 0.99 for the rank-1 model to 0.98, which indicates a slight deviation of the prepared states from the specified ones. At the same time, the further increase in the model rank to 3 does not affect the reconstruction accuracy, because only two crystals were used in the preparation scheme, which means that even in the case of incom-

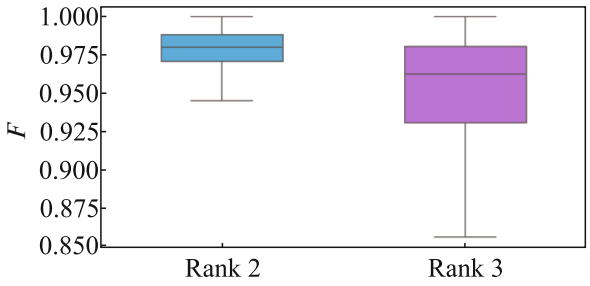

Fig. 5. (Color online) Fidelity distributions for the protocol A5 tomography of states of ranks 2 and 3.

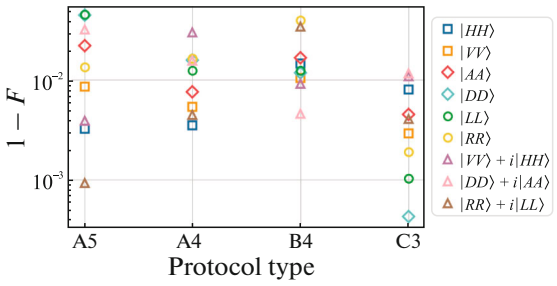

Fig. 6. (Color online) Experimental results for rank 1 reconstruction with the protocols under study.

plete interference, the rank of the prepared state cannot be larger than 2, and the rank-3 model is excessive.

To evaluate the effectiveness of the protocol A5 for the mixed-state tomography, we generated data corresponding to the results of measuring the states of ranks 2 and 3. For this purpose, density matrices were randomly generated, each matrix was represented in the form of the decomposition (8), and the measurement data were combined from the measurements of the states $\{|\phi_j\rangle\}$ in the relation determined by the coefficients a_j. For each rank, the results of measuring 10000 matrices were generated, their tomography was carried out, and fidelity values were calculated. The resulting fidelity distributions are shown in Figs. 5 and 8. It can be seen that the accuracy of the protocol decreases with increasing rank, because the number of parameters that need to be reconstructed increases, but the average fidelity value even for rank 3 is 0.96, which confirms the possibility of using this protocol for mixed-state tomography.

5. CONCLUSIONS

To summarize, the completeness of tomography protocols for polarization qutrits of various ranks has been examined. It has been shown that the protocol A5 consisting of five measurements presented in [24] is complete for states of any rank. The protocol B4 including four measurements is complete only for pure states, as stated by its authors [28]. It appears that the protocol A5 can also be reduced to the protocol A4, consisting of four measurements, which is complete for pure states. Moreover, the protocol C3 consisting of only three measurements that is also complete for pure states has been found. All the protocols under study have been tested in experiments and have demonstrated a high accuracy in reconstructing test states, and the errors seem to be related to the preparatory rather than the measuring part.

The results of the work can be directly used to debug quantum schemes using polarization qutrits, and the approaches used in the work can be applied to tomography problems of qudits of arbitrary nature.

APPENDIX A
MAXIMUM LIKELIHOOD TOMOGRAPHY ALGORITHM

Let n pairs of photons be prepared in the time interval t in a series of measurements, where $k_{\beta,0}$ events with no photons, $k_{\beta,1}$ events with the $|HH\rangle$ state, $k_{\beta,2}$ events with the $|HV\rangle$ state, and $k_{\beta,3}$ events with the $|VV\rangle$

Table 2. Fidelity of the protocols under study

Rank	$\|HH\rangle$	$\|VV\rangle$	$\|AA\rangle$	$\|DD\rangle$	$\|RR\rangle$	$\|LL\rangle$	$\|VV\rangle + \mathrm{i}\cdot\|\mathrm{HH}\rangle$	$\|DD\rangle + \mathrm{i}\cdot\|\mathrm{AA}\rangle$	$\|RR\rangle + \mathrm{i}\cdot\|\mathrm{LL}\rangle$
Fidelity of the protocol A5									
1	0.9968	0.9915	0.9928	0.9908	0.9939	0.9935	0.9961	0.9874	0.9991
2	0.9968	0.9915	0.9781	0.9554	0.9866	0.9550	0.9961	0.9682	0.9991
3	0.9968	0.9915	0.9781	0.9554	0.9866	0.9550	0.9961	0.9682	0.9991
Fidelity of the protocol A4									
1	0.9965	0.9946	0.9925	0.9843	0.9835	0.9876	0.9702	0.9844	0.9955
Fidelity of the protocol B4									
1	0.9985	0.9949	0.9909	0.9954	0.9910	0.9921	0.9937	0.9955	0.9938
Fidelity of the protocol C3									
1	0.9920	0.9971	0.9955	0.9994	0.9981	0.9989	0.9891	0.9884	0.9959

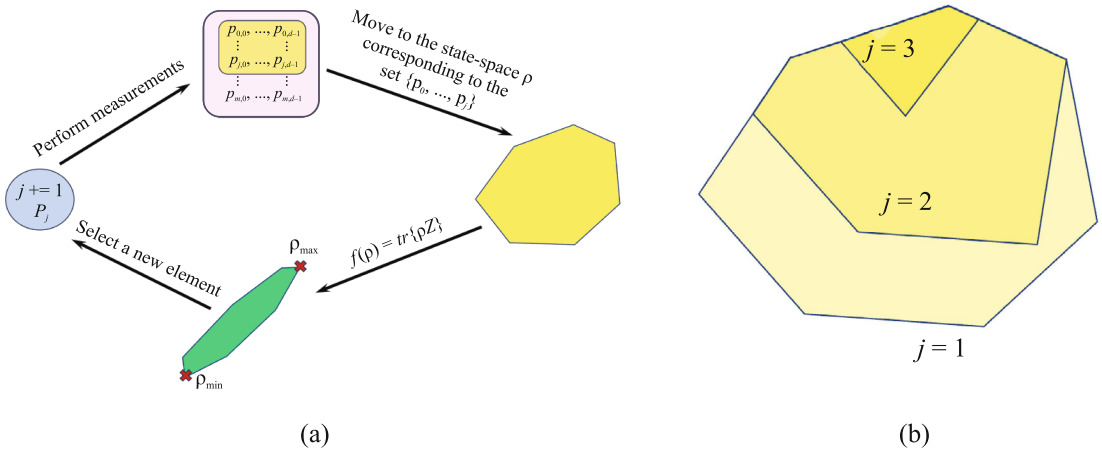

Fig. 7. (Color online) (a) Diagram of the iterative process of adaptive compressive tomography. (b) Contraction of the hyperplane with the iteration j.

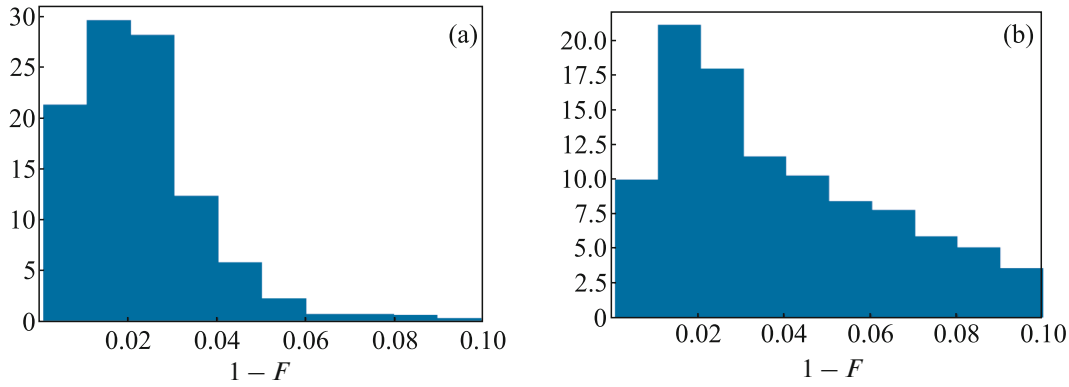

Fig. 8. (Color online) Distributions of the quantity $1 - F$ for the protocol A5 tomography of states of ranks (a) 2 and (b) 3.

state are detected, so that $n = k_{\beta,0} + k_{\beta,1} + k_{\beta,2} + k_{\beta,3}$. The probabilities of the outcomes are independent and satisfy the Poisson distribution with the parameters $\lambda_{\beta,i}$ [24]:

$$f(k_{\beta,i}) = \frac{(\lambda_{\beta,i})^{k_{\beta,i}}}{k_{\beta,i}!} e^{-\lambda_{\beta,i}}, \quad i = 1,2,3. \qquad \text{(A.1)}$$

Let ρ_0 be the result of solving Eq. (1) by the pseudo-inversion method with respect to the empirical probabilities $\hat{p}_{\beta,i} = k_{\beta,i}/\sigma_i$. Let us consider the spectral decomposition $\rho_0 = UDU^\dagger$, where U is the unitary matrix of eigenvectors and D is the diagonal matrix of real eigenvalues of ρ_0 (we assume that the eigenvalues are arranged in non-increasing order). Let us equate all the negative elements of the matrix D to zero and compose the matrix $\tilde{\psi}_0 = U\sqrt{D}$. Let the first r columns of this matrix compose the matrix ψ_0, which is then normalized as $\psi_0 \to \psi_0/\sqrt{\mathrm{Tr}\{\psi_0^\dagger\psi_0\}}$. The matrix $\psi_0\psi_0^\dagger$ is the density matrix in the zeroth approximation.

The matrix ψ_0 is in turn a good zeroth approximation for the more accurate maximum likelihood method of. In view of Eq. (A.1), the likelihood function is determined by the product of the Poisson probabilities:

$$L(\psi) = \prod_{\beta}\prod_{i=1}^{d} f(k_{\beta,i} \mid \lambda_{\beta,i}(\psi)),$$

$$\lambda_{\beta,i}(\psi) = \sigma_i \mathrm{Tr}\{P_{\beta,i}\psi\psi^\dagger\}.$$

It is more convenient to consider logarithmic likelihood (logarithm of the likelihood function):

$$\ln(L(\psi)) = \ln\left(\prod_{\beta}\prod_{i=1}^{d} f(k_{\beta,i} \mid \lambda_{\beta,i}(\psi))\right)$$

$$\propto \sum_{\beta}\sum_{i=1}^{d}[k_{\beta,i}\ln\lambda_{\beta,i} - \lambda_{\beta,i}].$$

The term $\ln(k_{\beta,j}!)$ does not affect the position of the extremum and can be neglected. Equating the minimum of this function to zero, we get

$$\sum_{\beta}\sum_{i=1}^{d}\left(\frac{k_{\beta,i}}{\lambda_{\beta,i}} - 1\right)\sigma_i P_{\beta,i}\psi = 0.$$

Let us perform the change

$$A(\psi) = \sum_{\beta}\sum_{i=1}^{d}\left(\frac{k_{\beta,i}}{p_{\beta,i}}\right)P_{\beta,i}, \quad Q = \sum_{\beta}\sum_{i=1}^{d}\sigma_i P_{\beta,i}.$$

Then, we obtain a nonlinear equation $Q^{-1}A(\psi)\psi = \psi$, which can be solved with respect to ψ using the simple iterative method. The resulting density matrix of rank no more than r is then calculated by the formula $\rho = \psi\psi^{\dagger}/\mathrm{Tr}\{\psi^{\dagger}\psi\}$. Such root parameterization guarantees that the resulting density matrix is physical.

APPENDIX B

STATE PURIFICATION PROCEDURE AND INFORMATION MATRIX

First, we consider the state purification procedure [29]. Let the $d \times d$ density matrix ρ of the rank r have the eigenvectors c_κ and eigenvalues μ_κ. Then, instead of the initial density matrix, we can consider a "purified" state vector of the form

$$c = \begin{pmatrix}\sqrt{\mu_1}c_1\\ \vdots \\ \sqrt{\mu_r}c_r\end{pmatrix}.$$

The amplitude of the quantum process for the pure state ($r = 1$) can be represented as:

$$M_\kappa = X_\kappa|c\rangle,$$

where X_κ is the κth line for the protocol measurement P. In the case of a purified state, this line is generalized as

$$X_\kappa^l = |e^l\rangle^{\dagger}\otimes X_\kappa,$$

where $|e^l\rangle$ are orthonormalized basic states. For the rank r, we assume

$$|e^1\rangle = \begin{pmatrix}1\\0\\\vdots\\0\\0\end{pmatrix}, \quad |e^2\rangle = \begin{pmatrix}0\\0\\\vdots\\0\\0\end{pmatrix},\ldots,$$

$$|e^{r-1}\rangle = \begin{pmatrix}0\\0\\\vdots\\1\\0\end{pmatrix}, \quad |e^r\rangle = \begin{pmatrix}0\\0\\\vdots\\0\\1\end{pmatrix}.$$

The intensity of event generation (the expected number of events in the scheme per unit time) can be expressed in terms of the amplitude of the quantum process as

$$\gamma_\kappa = M_\kappa^{\dagger}M_\kappa = \langle c|\Lambda_\kappa|c\rangle,$$

from which the process intensity operator follows in the form

$$\Lambda_\kappa = \sum_{l=1}^{r}\left(X_\kappa^l\right)^{\dagger}X_\kappa^l.$$

Note that the equality $\lambda_\kappa = \gamma_\kappa t_\kappa$, where t_κ is the exposure time, is valid for our experiment. We now pass from complex vectors and matrices to real ones as follows:

$$c \to \begin{pmatrix}\mathrm{Re}(c)\\ \mathrm{Im}(c)\end{pmatrix}, \quad M \to \begin{pmatrix}\mathrm{Re}(M)\\ \mathrm{Im}(M)\end{pmatrix},$$

$$X_\kappa^l \to \begin{pmatrix}\mathrm{Re}(X_\kappa^l) & -\mathrm{Im}(X_\kappa^l)\\ \mathrm{Im}(X_\kappa^l) & \mathrm{Re}(X_\kappa^l)\end{pmatrix}.$$

The discrepancy between the exact state vector and its reconstruction should be interpreted as a manifestation of statistical fluctuations that inevitably arise due to the fundamentally probabilistic nature of quantum mechanics. The quantitative characteristic of such fluctuations is given by the matrix of complete information, which is introduced in [21, 29] and corresponds in our notation to Eq. (3). If $|dc\rangle$ is the difference between the exact and reconstructed vectors, the level of statistical fluctuations is described by the quantity

$$2\langle dc|H|dc\rangle = \chi^2(2dr - r^2).$$

Then, if the protocol is complete, the symmetric real matrix H has exactly $2dr - r^2$ positive eigenvalues. In this case, the remaining r^2 eigenvalues are zero.

APPENDIX C

ADAPTIVE COMPRESSIVE TOMOGRAPHY ALGORTIM

The adaptive compressive tomography algorithm described in [11–13] is presented below.

We verify the completeness of the protocol $P = \{P_1, P_2, \ldots, P_m\}$ consisting of m measurements for a state with a known rank r. First, we choose an arbitrary measurement P_j, where j is the iteration process number; therefore, initially $j = 1$. We generate the $d \times d$

density matrix ρ of the rank r, and an arbitrary $d \times d$ complex matrix Z needed below. The numerical simulation was performed with a function generating $d \times d$ random matrices of a given rank r. The elements of the matrix $Q \in \mathbb{C}^{r\times d}$ are specified as the sum of normally distributed random independent real and imaginary parts: $Q_{ab} = X_{ab} + iY_{ab}$, where $X_{ab}, Y_{ab} \sim \mathcal{N}(0,1/2)$. The obtained positively defined matrix is constructed in the form

$$\rho = \frac{Q^\dagger Q}{\mathrm{Tr}\{Q^\dagger Q\}},$$

which ensures that the density matrix ρ has the unit trace and a given rank r. As the initial conditions of the algorithm, 500 such matrices are used. The iterative process is described as follows (see Fig. 7).

(i) The measurement frequencies $\sum_{l=0}^{d-1} k_{lj} = 1$ are calculated for the selected measurement P_j and the density matrix ρ.

(ii) Using these frequencies k_{lj} and the maximum likelihood method, we obtain the reconstructed density matrix R.

(iii) We introduce the function $f(R) = \mathrm{Tr}\{ZR\}$ and $s_{\mathrm{cvx}} = (f_{\max,j} - f_{\min,j})/(f_{\max,1} - f_{\min,1})$. It can be proved that the protocol is informationally complete if $f_{\max,j} = f_{\min,j}$. Therefore, the protocol is complete at $s_{\mathrm{cvx}} = 0$ (but $s_{\mathrm{cvx}} \approx 0$ for numerical calculation).

(iv) The parameter s_{cvx} is calculated. If $s_{\mathrm{cvx}} \approx 0$, the iterative process can be stopped; otherwise, another measurement is selected and items (i)–(iii) are repeated for the set $\{P_1, \ldots, P_{j+1}\}$.

Note:

(i) To randomly generate the initial density matrix ρ with a given rank r, a matrix A of the dimension $r \times d$ is generated, and the density matrix is obtained as

$$\rho = \frac{A^\dagger A}{\mathrm{Tr}\{A^\dagger A\}}.$$

(ii) The matrix Z should be full-rank to avoid some critical cases, for example,

(a) $Z = 1/d$; in this case, $f(\rho) = 1$ for any ρ;

(b) $Z = |\psi\rangle\langle\psi|$, where $|\psi\rangle$ can be such a pure state that $s_{\mathrm{cvx}} = 0$ for any ρ.

(iii) The von Neumann entropy $S(\rho^*) = -\mathrm{Tr}\{\rho^* \log(\rho^*)\}$ or linear entropy $S(\rho^*) = 1 - \mathrm{Tr}\{(\rho^*)^2\}$ can be used to choose the next measurement P_{j+1}. Then, item (v) will be added to the iterative algorithm, where ρ_a^* should first be found at which $S(\rho_a^*)$ is minimal. Then, P_{j+1} closest to the natural basis ρ_a^* is chosen. This method is best used in multiparticle systems, because it simplifies the experimental implementation of the obtained bases, but can simultaneously increase their number and, accordingly, the measurement time.

ACKNOWLEDGMENTS

We are grateful to M.V. Fedorov for fruitful discussions.

FUNDING

This work was supported by the Russian Science Foundation (project no. 22-12-00263-P, https://rscf.ru/project/22-12-00263/).

CONFLICT OF INTEREST

The authors of this work declare that they have no conflicts of interest.

REFERENCES

1. M. A. Nielsen and I. L. Chuang, *Quantum Computation and Quantum Information,* 10th ed. (Cambridge Univ. Press, Cambridge, UK, 2010).
2. H. J. Kimble, "The quantum internet," Nature (London, U.K.) **453**, 1023 (2008).
3. M. Erhard, R. Fickler, M. Krenn, and A. Zeilinger, "Experimental Greenberger–Horne–Zeilinger entanglement beyond qubits," Phys. Rev. Lett. **123**, 070505 (2019).
4. M. Ringbauer, M. Meth, L. Postler, R. Stricker, R. Blatt, Ph. Schindler, and Th. Monz, "A universal qudit quantum processor with trapped ions," Nat. Phys. **18**, 1053 (2022).
5. Y. Jo, T. Jeong, N. H. Park, Z. Kim, D.-G. Im, K. Park, and Y. S. Ihn, "Security analysis of qutrit quantum secret sharing with linear optical correlation measurement," Sci. Rep. **15**, 19836 (2025).
6. I. V. Zalivako, A. S. Nikolaeva, A. S. Borisenko, A. E. Korolkov, P. L. Sidorov, K. P. Galstyan, N. V. Semenin, V. N. Smirnov, M. A. Aksenov, K. M. Makushin, E. O. Kiktenko, A. K. Fedorov, I. A. Semerikov, K. Yu. Khabarova, and N. N. Kolachevsky, "Towards a multiqudit quantum processor based on a $^{171}Yb^+$ ion

string: Realizing basic quantum algorithms," Quantum Rep. **7** (2), 19 (2025).

7. W. K. Wootters and B. D. Fields, "Optimal state determination by mutually unbiased measurements," Ann. Phys. **191**, 363 (1989).
8. T. Durt, B.-G. Englert, I. Bengtsson, and K. Zyczkowski, "On mutually unbiased bases," Int. J. Quantum Inf. **8**, 535 (2010).
9. T. Heinosaari, L. Mazzarella, and M. M. Wolf, "Quantum tomography under prior information," Commun. Math. Phys. **318**, 355 (2013).
10. D. Gross, Y.-K. Liu, S. T. Flammia, S. Becker, and J. Eisert, "Quantum state tomography via compressed sensing," Phys. Rev. Lett. **105**, 150401 (2010).
11. D. Ahn, Y. S. Teo, H. Jeong, F. Bouchard, F. Hufnagel, E. Karimi, D. Koutný, J. Řeháček, Z. Hradil, G. Leuchs, and L. L. Sánchez-Soto, "Adaptive compressive tomography with no a priori information," Phys. Rev. Lett. **122**, 100404 (2019).
12. D. Ahn, Y. S. Teo, H. Jeong, D. Koutný, J. Řeháček, Z. Hradil, G. Leuchs, and L. L. Sánchez-Soto, "Adaptive compressive tomography: A numerical study," Phys. Rev. A **100**, 012346 (2019).
13. Y. S. Teo, G. I. Struchalin, E. V. Kovlakov, D. Ahn, H. Jeong, S. S. Straupe, S. P. Kulik, G. Leuchs, and L. L. Sánchez-Soto, "Objective compressive quantum process tomography," Phys. Rev. A **101**, 022334 (2020).
14. S. T. Flammia, A. Silberfarb, and C. M. Caves, "Minimal informationally complete measurements for pure states," Found. Phys. **35**, 1985 (2005).
15. Y. Wang and J. Shang, "Pure state really informationally complete with rank-1 POVM," Quantum Inform. Process. **17**, 51 (2018).
16. C. Carmeli, T. Heinosaari, J. Schultz, and A. Toigo, "How many orthonormal bases are needed to distinguish all pure quantum states?," Eur. Phys. J. D **69**, 1 (2015).
17. C. Carmeli, T. Heinosaari, M. Kech, J. Schultz, and A. Toigo, "Stable pure state quantum tomography from five orthonormal bases," Europhys. Lett. **115**, 30001 (2016).
18. A. V. Burlakov, M. V. Chekhova, O. A. Karabutova, D. N. Klyshko, and S. P. Kulik, "Polarization state of a biphoton: Quantum ternary logic," Phys. Rev. A **60**, R4209 (1999).
19. A. V. Burlakov, L. A. Krivitski, S. P. Kulik, G. A. Maslennikov, and M. V. Chekhova, "Measurement of qutrits," Opt. Spectrosc. **94**, 684 (2002).
20. Yu. I. Bogdanov, M. V. Chekhova, S. P. Kulik, G. A. Maslennikov, A. A. Zhukov, C. H. Oh, and M. K. Tey, "Qutrit state engineering with biphotons," Phys. Rev. Lett. **93**, 230503 (2004).
21. Yu. I. Bogdanov, M. V. Chekhova, L. A. Krivitsky, S. P. Kulik, A. N. Penin, A. A. Zhukov, L. Ch. Kwek, Ch. H. Oh, and M. K. Tey, "Statistical reconstruction of qutrits," Phys. Rev. A **70**, 042303 (2004).
22. B. P. Lanyon, T. J. Weinhold, N. K. Langford, J. L. O'Brien, K. J. Resch, A. Gilchrist, and A. G. White, "Manipulating biphotonic qutrits," Phys. Rev. Lett. **100**, 060504 (2008).
23. S. P. Kulik and S. S. Straupe, "Entanglement of biphoton-based qutrits and ququarts," Laser Phys. **24**, 94007 (2014).
24. N. A. Borshchevskaya, D. R. Chupakhin, B. I. Bantysh, K. G. Katamadze, S. P. Kulik, and Yu. I. Bogdanov, "Tomography of polarization qutrits in the standard basis," Radiophys. Quantum Electron. **67**, 64 (2024).
25. J. Finkelstein, "Pure-state informationally complete and really complete measurements," Phys. Rev. A **70**, 052107 (2004).
26. Yu. I. Bogdanov, "Unified statistical method for reconstructing quantum states by purification," J. Exp. Theor. Phys. **108**, 928 (2009).
27. S. Diamond and S. Boyd, "CVXPY: A python embedded modeling language for convex optimization," J. Mach. Learn. Res. **17** (83), 1 (2016).
28. M. V. Fedorov, C. C. Mernova, and K. V. Sliporod, "A protocol of measurements providing direct, complete and single-valued recover of all a-priori unknown parameters of biphoton polarization qutrits," arXiv: 2401.15137 (2024).
29. Yu. I. Bogdanov, "Statistical inverse problem: Root approach," quant-ph/0312042 (2003).

Translated by R. Tyapaev